

GraL spectroscopic identification of multiply imaged quasars

Priyanka JALAN^{1,*}, Vibhore NEGI², Jean SURDEJ³, Céline BOEHM⁴,
 Ludovic DELCHAMBRE³, Jakob Sebastian DEN BROK⁵, Dougal DOBIE⁶, Andrew DRAKE⁷,
 Christine DUCOURANT⁸, S. George DJORGOVSKI⁷, Laurent GALLUCCIO⁹,
 Matthew J. GRAHAM⁷, Jonas KLÜTER^{10,11}, Alberto KRONE-MARTINS^{12,13},
 Jean-François LECAMPION⁸, Ashish A. MAHABAL⁷, François MIGNARD⁹, Tara MURPHY⁶,
 Anna NIERENBERG¹⁴, Sergio SCARANO¹⁵, Joseph SIMON¹⁴, Eric SLEZAK⁹,
 Dominique SLUSE³, Carolina SPÍNDOLA-DUARTE¹⁶, Daniel STERN¹⁴,
 Ramachrisna TEIXERA¹⁶ and Joachim WAMBSGANSS^{10,17}

¹ Center for Theoretical Physics, Polish Academy of Sciences, al. Lotników 32/46, 02-668 Warsaw, Poland

² Aryabhata Research Institute of Observational Sciences, Nainital, Uttarakhand, India

³ Institut d’Astrophysique et de Géophysique, Université de Liège, Allée du 6 Août 19c, B-4000 Liège, Belgium

⁴ School of Physics, The University of Sydney, NSW 2006, Australia

⁵ Sydney Institute for Astronomy, School of Physics, University of Sydney, NSW 2006, Australia

⁶ Argelander-Institut für Astronomie, Universität Bonn, Auf dem Hügel 71, D-53121 Bonn, Germany

⁷ Cahill Center for Astronomy and Astrophysics, California Institute of Technology, 1216 E. California Blvd., Pasadena, CA 91125, US

⁸ Laboratoire d’Astrophysique de Bordeaux, Univ. Bordeaux, CNRS, B18N, allée Geoffroy Saint-Hilaire, 33615 Pessac, France

⁹ Université Côte d’Azur, Observatoire de la Côte d’Azur, CNRS, Laboratoire Lagrange, Boulevard de l’Observatoire, CS 34229, 06304 Nice, France

¹⁰ Zentrum für Astronomie der Universität Heidelberg, Astronomisches Rechen-Institut, Mönchhofstr. 12-14, 69120 Heidelberg, Germany

¹¹ Department of Physics & Astronomy, Louisiana State University, 261 Nicholson Hall, Tower Dr., Baton Rouge, LA 70803-4001, US

¹² Donald Bren School of Information and Computer Sciences, University of California, Irvine, Irvine CA 92697, US

¹³ CENTRA, Faculdade de Ciências, Universidade de Lisboa, 1749-016, Lisbon, Portugal

¹⁴ Jet Propulsion Laboratory, California Institute of Technology, 4800 Oak Grove Drive, Mail Stop 264-789, Pasadena, CA 91109, USA

¹⁵ Departamento de Física - CCET, Universidade Federal de Sergipe, Rod. Marechal Rondon s/n, 49.100-000, Jardim Rosa Elze, São Cristóvão, SE, Brazil

¹⁶ Instituto de Astronomia, Geofísica e Ciências Atmosféricas, Universidade de São Paulo, Rua do Matão, 1226, Cidade Universitária, 05508-900 São Paulo, SP, Brazil

Abstract

Gravitational lensing is proven to be one of the most efficient tools for studying the Universe. The spectral confirmation of such sources requires extensive calibration. This paper discusses the spectral extraction technique for the case of multiple source spectra being very near each other. Using the *masking technique*, we first detect high Signal-to-Noise (S/N) peaks in the CCD spectral image corresponding to the location of the source spectra. This technique computes the cumulative signal using a weighted sum, yielding a reliable approximation for the total counts contributed by each source spectrum. We then proceed with the subtraction of the contaminating spectra. Applying this method, we confirm the nature of 11 lensed quasar candidates.

Keywords: Quasar, gravitational lensing, spectroscopy, multiply imaged quasars

1. Introduction

The two chief methods for estimating the Hubble-Lemaître constant (H_0) are (i) studying the relation between the distances and redshifts of the objects in the Universe (see, e.g., Lemaître, 1927; Hubble, 1929), (ii) interpolating the expansion rate from models based on the Cosmic Microwave Background Radiation (see, e.g., Efstathiou et al., 1990; Jimenez et al., 2003) and Type-1a supernovae (see, e.g., Riess et al., 1998; Perlmutter et al., 1999). However, studying gravitational lens systems has proven to be a complementary tool to determine H_0 in a model-independent manner (see, e.g., Refsdal, 1964; Blandford and Narayan, 1992; Surdej and Refsdal, 1994; Kelly et al., 2023).

Gravitational lensing is due to the deflection of light from a background source caused by a massive foreground structure (see, e.g., Fig. 1). The mass of the foreground source leads to a curved space-time that bends the light travelling from the background source to the observer. The deflection of light depends on the distribution of mass within the foreground structure and the distances between the observer, the lens and the source. Such lensing can produce multiple images and/or amplification of the background source. The delay between the light travel times corresponding to the various lensed images contains information about H_0 . In addition to the estimation of H_0 , gravitational lens systems can also be used to evaluate the mass of the foreground structure as well as properties of dark energy and matter (see, e.g., Cao et al., 2015, and references therein). Furthermore, the transverse correlation of the Ly α forest clouds in the IGM can also be studied using gravitationally lensed quasars (Bechtold and Yee, 1995; Dolan et al., 2000; Rauch et al., 2001; Tzanavaris and Carswell, 2003).

The concept of gravitational lensing is traced back to 1704 when Newton, in his work *Opticks*, questions whether objects may interact with light at a distance and bend the light beams. It was in 1784 that Henry Cavendish, using Newton’s gravitational theory and Newtonian optics, computed the deflection angle of light due to a point mass, where light is supposed

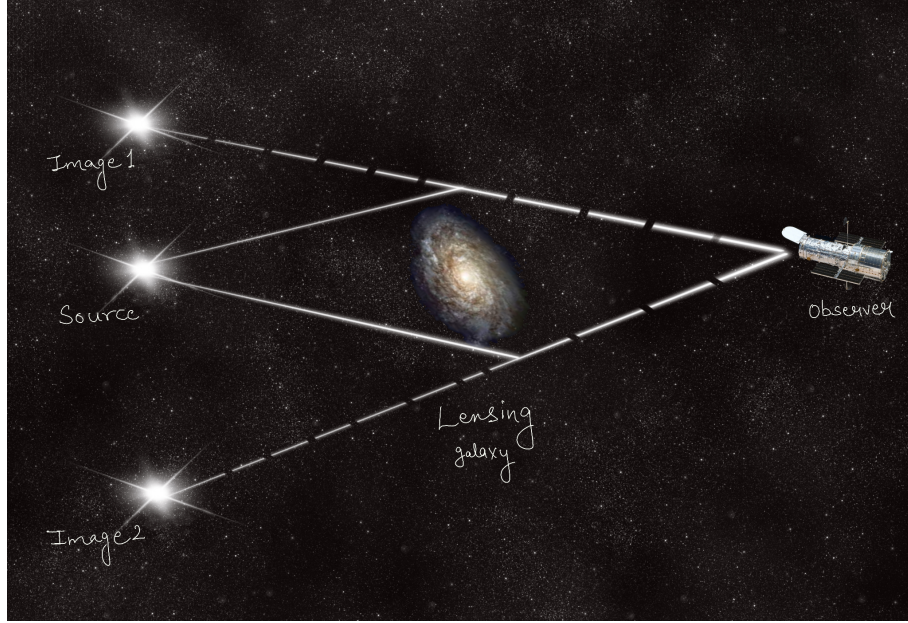


Figure 1: This artistic image shows light deflection from a background quasar due to a foreground galaxy producing two lensed images of the quasar.

to be composed of corpuscles being affected by a gravitational field in the same way as material particles (detailed in Lotze and Simionato, 2022). Later, Johann Georg von Soldner calculated the angle of deflection of light passing at a distance ‘ b ’ from a mass M as,

$$\alpha_N = \frac{2GM}{c^2 b}. \quad (1)$$

here, G is the gravitational constant, and c is the speed of light in a vacuum.

In 1915, Albert Einstein calculated the deflection angle of light by the Sun using his general theory of relativity and found that this angle was twice that previously predicted. In 1937, Fritz Zwicky (Zwicky, 1937) argued that this phenomenon might let galaxy clusters serve as gravitational lenses. It was not until 1979 that the detection of the twin quasars SBS 0957+561 by Walsh et al. (1979) was shown to be the first example of a doubly imaged quasar.

The discovery of such exotic sources requires overcoming various observational challenges. Not only are these objects rare, but they are also challenging to be identified in large catalogues. Therefore, only two hundreds of spectroscopically confirmed gravitational systems (<https://research.ast.cam.ac.uk/lensedquasars/index.html>) are currently known. Recent studies have tried discovering these systems using machine learning algorithms and large astronomical surveys. One such effort is made by the Gaia-GraL (Gaia Gravitational Lens systems) group using the Gaia data, an all-sky survey space-based mission designed to catalogue the stars in the Milky Way. However, while doing so, various extragalactic sources are also unveiled in this process (Tsalmantza et al., 2012; Krone-Martins et al., 2013; de Souza et al., 2014; Delchambre, 2018; Bailer-Jones et al., 2019; Creevey et al., 2023). The best angular resolution of $0.18''$ achievable with Gaia does provide an excellent opportunity to search for gravitational lens can-

didates (Agnello et al., 2018; Lemon et al., 2018). Finet and Surdej (2016) have predicted to find ~ 2900 such lensed quasar candidates in the Gaia survey. Since then the Gaia-GraL team has spectroscopically confirmed 15 quadruply imaged systems and seven doubly ones (see, e.g., Krone-Martins et al., 2018; Ducourant et al., 2018; Delchambre et al., 2019; Wertz et al., 2019; Krone-Martins et al., 2019; Stern et al., 2021).

In this paper, we discuss one of the data reduction techniques developed to spectroscopically confirm these sources to be gravitationally lensed quasars.

2. Observations

The spectroscopic observations of the gravitationally lensed candidates were performed using EFOSC2 installed at the New Technology Telescope (<https://www.eso.org/sci/facilities/lasilla/instruments/efosc.html>) and ADFOSC equipping the 3.6 m Devasthal Optical Telescope (<https://www.aries.res.in/facilities/astronomical-telescopes/360cm-telescope/Instruments>).

3. Spectroscopy

The extraction process that uses the `apa11` task in IRAF is quite simple if the two nearby source spectra are well separated. However, for most of the gravitational lens systems, the multiple lensed quasar images are very near each other, complicating the extraction process of individual non-contaminated spectra (e.g., left panel of Fig. 2). When extracting the spectrum of a designated source component, it is important to subtract the contamination due to all the other ones correctly. The right panel of Fig. 2 shows counts versus pixel numbers along a fixed row of the CCD spectral image illustrated in the left panel. Firstly, we assume a *Gaussian distribution* of the photon counts from a source for a particular CCD row, i.e., the point spread function (PSF). Therefore, we have over-plotted two Gaussian profiles associated with the two nearby spectra (say due to component C_1 and component C_2) along with the background in cyan colour. In the right panel of Fig. 2, the red colour represents the contaminated area by the neighbouring source. The region of C_2 contaminating the flux of C_1 is similar to sub_1 (shown in orange dashed lines). Similarly, the region of C_1 contaminating the flux of C_2 is similar to sub_2 (shown in green dashed lines). So in order to retain uncontaminated spectra,

$$C_1^{decont} = C_1^{cont} - sub_1 ; C_2^{decont} = C_2^{cont} - sub_2. \quad (2)$$

The extraction using IRAF gives good results for bright and well-separated sources; however, faint and very nearby sources require a more intricate extraction technique.

3.1. Decontamination of nearby spectra

Masking technique: The optimal spectral extraction that we propose makes use of a *masking technique*, as briefly discussed below. This technique is advantageous in the case of doubly imaged quasars for which both spectra lie very close to each other and significantly contaminate

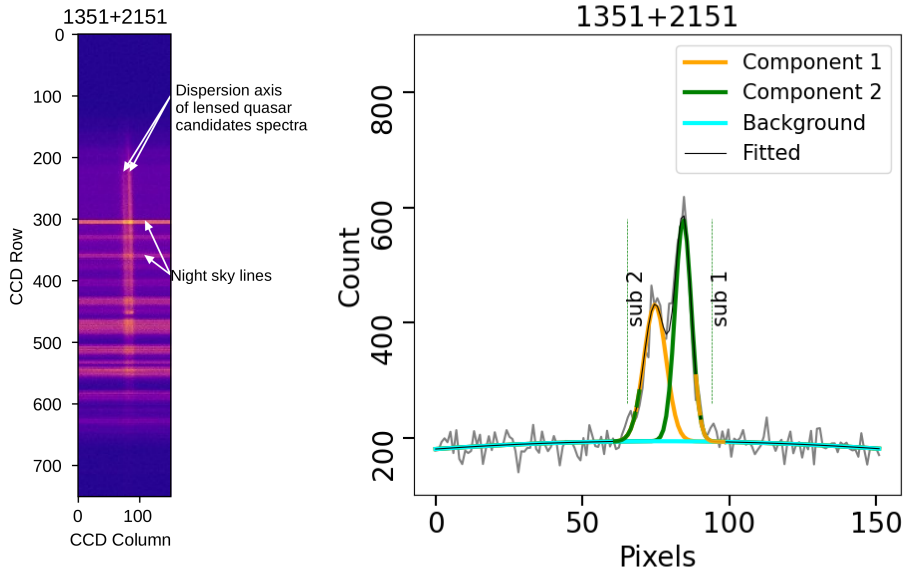


Figure 2: *Left:* CCD frame highlighting the spectra of two nearby lensed quasar images and superimposed night skylines. *Right:* Slice of the CCD along row number 270 shows the superposition of two almost Gaussian profiles. In Section 3.1, the technique to remove the contamination of neighbouring sources is detailed.

each other. Also, this algorithm is highly useful in reducing the statistical noise of the extracted spectra by assigning non-uniform pixel weights during the extraction.

- [1] After pre-processing the science image, the CCD image ($I_* + Sky$), as shown in the left panel of Fig. 2, is used to create several other images (see below).
- [2] The background image (Sky) is created after applying a sigma clipping algorithm to the spectra along each row. The sky array is the median of the remaining pixels along each row. We then subtract from each column this median sky background.
- [3] We then generate a binary mask, which in the case of a single source, would mimic the shape of the displayed source spectrum. We assign the value of 1 to each pixel inside the mask and 0 everywhere else. In the case of a double source spectrum, we construct the mask by fitting, at best, its shape to that of the brightest source spectrum.
- [4] The mask is then multiplied with the science image step-[1] generating the $(I_* + Sky)_M$ masked image (the subscript M indicates that the frame has been masked).
- [5] We also multiply the mask with the background subtracted image step-[2], leading to $(I_*)_M$.
- [6] Using the gain and readout-noise (Ron) of the CCD, the noise at the i^{th} pixel is calculated as $N_i = \sqrt{\frac{(I_* + Sky)_{iM}}{gain} + Ron_{ADU}^2}$.

- [7] Step-[5] and step-[6] lead to the estimation of the relative weight w_i at each pixel of the CCD: $w_i = (I_*)_{iM}/N_i^2$.
- [8] The above weights are summed up along the row: $\sum_{i=0}^n (I_*)_{iM}/N_i^2$.
- [9] Normalizing the weight w_i of the pixels along the rows, we find that $W_i = \frac{(I_*)_{iM}/N_i^2}{\sum_{i=0}^n (I_*)_{iM}/N_i^2}$.
- [10] These weights are then multiplied with the signal step-[5] i.e, $W_i \times (I_*)_{iM}$.
- [11] Remember, the masking has led to zero values elsewhere but unity within the mask width. Therefore, a sum of the weighted signal along the row will give the total signal $S = \sum W_i \times (I_*)_{iM}$. This process leads to a one-dimensional extracted spectrum having a length equal to that of the CCD columns.
- [12] In order to calculate the total noise, we multiply the weights with the noise step-[6], i.e., $W_i^2 \times N_i^2$.
- [13] Similar to step-[10], the total noise along the mask width is $N = \sqrt{\sum W_i^2 \times N_i^2}$. Similar to the signal spectrum, a one-dimensional noise spectrum with a length equal to that of the CCD columns is generated.
- [14] Finally, we slide the mask along the rows, and for each column position, we calculate the corresponding S/N quantity. The presence of a source spectrum leads to a maximum value for S/N. The presence of two extrema (at positions X_1 and X_2) corresponds to the signature of two source spectra present on the CCD frame (see Fig. 3).
- [15] After detecting such peaks, the above process is repeated for various mask widths in order to optimally extract the spectra ($I[X_1]$ and $I[X_2]$). These are shown in blue colour in Fig. 4.
- [16] We also extract the spectra at positions $X_1 - (X_2 - X_1)$ and at positions $X_2 + (X_2 - X_1)$ (orange colour in Fig. 4) and then construct the following de-contaminated spectra: $I_D[X_1] = I[X_1] - I[X_2 + (X_2 - X_1)]$ and $I_D[X_2] = I[X_2] - I[X_1 - (X_2 - X_1)]$.

Fig. 3 shows two S/N peaks using the *masking technique* for the corresponding spectra shown in the left panel of Fig. 2. As seen from Fig. 4, the contaminated and decontaminated spectra look quite different.

4. Data log and results

The masking technique for removing the contamination of very closely separated quasars provides a unique method to extract the spectra of doubly imaged quasar candidates. Table 1 lists the sources for which the spectra have been extracted in this paper and were confirmed to be lensed. Out of 57 sources, we have confirmed 11 sources to be gravitationally lensed quasars. Ten of the 11 sources are doubly imaged quasars, whereas one quasar is a quadruply imaged quasar. The spectra are provided at https://github.com/PriyankaJalan14/Lens_spectra.

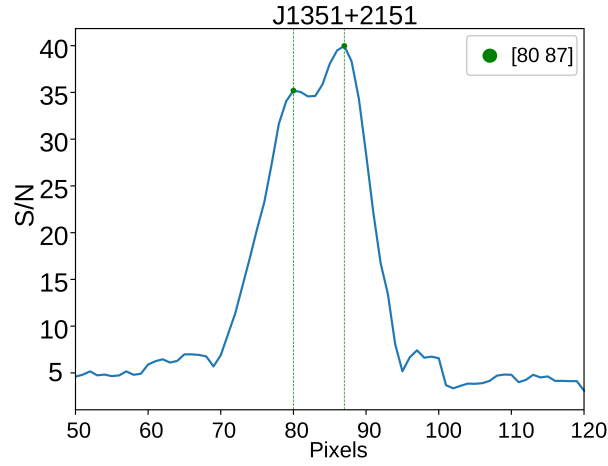


Figure 3: S/N versus pixel number for the CCD image shown in the left panel of Fig. 2.

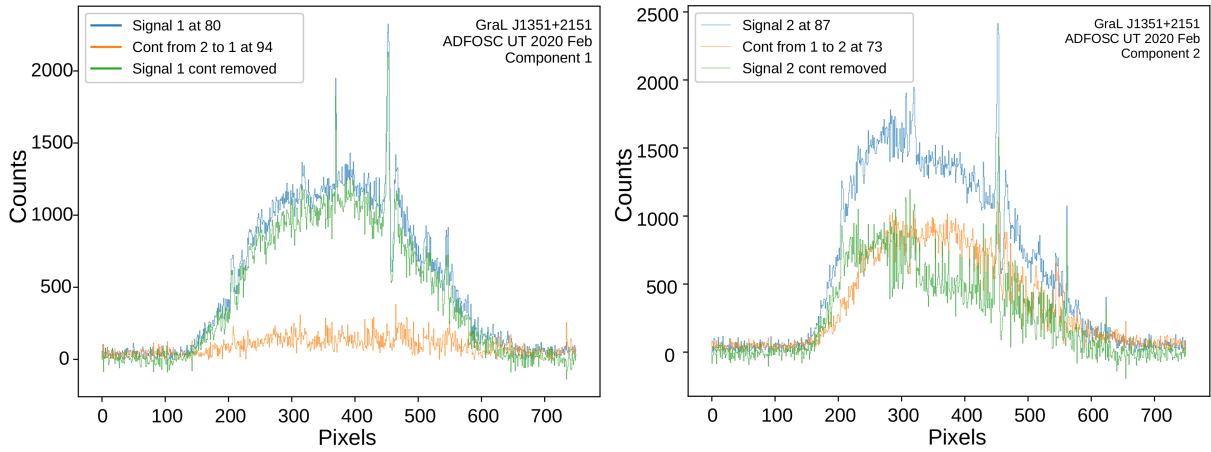


Figure 4: The blue spectra are those extracted at positions $X_1 = 80$ and $X_2 = 87$ from the spectral CCD frame shown in Fig. 2. The flux from the contamination at positions $X_1 - (X_2 - X_1)$ and at positions $X_2 + (X_2 - X_1)$ are orange. The decontaminated spectra $I_D[X_1] = I[X_1 = 80] - I[X_2 + (X_2 - X_1) = 94]$ and $I_D[X_2] = I[X_2 = 87] - I[X_1 - (X_2 - X_1) = 73]$ are shown in green colour.

Table 1: Observation log of the gravitational lens candidates. The lensing nature is also confirmed in the quoted references.

Quasar	Date	For each component			Lens confirmation	
		Telescope	RA	DEC		m_r
0013+5119	10-01-2021	DOT	00:13:23.5	+51:19:05.9	21.43	Probable lensed QSO [Lemon et al. 2019]
			00:13:23.5	+51:19:04.6	20.79	
			00:13:23.6	+51:19:07.5	20.52	
0645−1929	10-01-2021	DOT	06:45:44.0	−19:29:36.6	21.13	Doubly imaged QSO
			06:45:44.1	−19:29:35.7	21.22	
			06:45:44.1	−19:29:37.6	19.10	
0803+3908	10-01-2021	DOT	08:03:57.7	+39:08:23.9	18.84	Doubly imaged QSO
			08:03:57.7	+39:08:23.1	19.71	
			08:03:57.8	+39:08:23.1	18.26	
0859−3011	08-04-2019	NTT	08:59:11.9	−30:11:34.7	20.23	Doubly imaged QSO
			08:59:11.9	−30:11:34.6	20.99	
			08:59:11.9	−30:11:35.4	20.87	
0911+0550	09-04-2019	NTT	09:11:27.6	+05:50:54.8	19.74	Doubly imaged QSO [Delchambre et al. 2019]
			09:11:27.6	+05:50:53.9	19.50	
1008−2215	22-02-2020	NTT	10:08:53.5	−22:15:16.9	20.53	Doubly imaged QSO
			10:08:53.5	−22:15:17.9	20.94	
			10:08:53.6	−22:15:18.2	19.75	
1124+5710	19-03-2021	DOT	11:24:55.3	+57:10:56.6	18.46	Doubly imaged QSO
			11:24:55.5	+57:10:58.1	19.76	
1145−0850	11-02-2021	DOT	11:45:26.0	−08:50:06.4	21.68	Probable lensed QSO
			11:45:25.9	−08:50:07.5	21.28	
			11:45:24.0	−08:50:04.0	20.62	
1554−2818	23-02-2020	NTT	15:54:2.3	−28:18:36.4	19.49	Doubly imaged QSO
			15:54:2.2	−28:18:34.6	19.99	
			15:54:2.2	−28:18:35.6	19.76	
1651−0417	09-04-2019	NTT	16:51:04.5	−04:17:25.0	20.29	Quadruply imaged QSO [Stern et al. 2021]
			16:51:05.5	−04:17:27.3	19.48	
			16:51:05.1	−04:17:27.8	18.98	
			16:51:05.2	−04:17:23.2	20.04	
1654+3318	13-02-2021	DOT	16:54:23.5	+33:18:02.9	20.82	Probable lensed QSO
			16:54:23.4	+33:18:02.2	20.83	
			16:54:23.5	+33:18:03.1	20.50	

5. Conclusions

The Gaia GraL group aims at discovering more gravitationally lensed quasars. The challenge is to remove the spectral contamination due to the proximity of the lensed images. An

optimized extraction technique is required to remove the contamination. In this paper, we have discussed the spectral extraction technique for the case of very nearby lensed components. We detect the high S/N peaks in the CCD image using a *masking technique*. This technique computes the cumulative signal using a weighted sum, yielding a reliable approximation for the total counts. We then subtract the mutual spectral contamination due to the proximity of the lensed images. The width of the mask is decided through an iterative process. In this paper, we have efficiently extracted the spectra to confirm/refute 57 quasar lens candidates using this technique. Out of fifty-seven candidates, 11 of them are found to be lensed quasars.

Acknowledgments

This work is partially based on the observations obtained at the 3.6m Devasthal Optical Telescope (DOT) under programme ID DOT-2020-C2-P49, DOT-2020-C2-P50, DOT-2020-C2-P54, DOT-2020-C2-P59, DOT-2021-C1-P11, DOT-2021-C1-P12, DOT-2021-C1-P17, DOT-2021-C1-P33, which is a National Facility run and managed by Aryabhata Research Institute of observational sciencES (ARIES), an autonomous Institute under the Department of Science and Technology, Government of India. The observations are also based on the European Organisation for Astronomical Research in the Southern Hemisphere under ESO programme(s) P103.A-0077, P104.A-575, P105.A-205, P106.A.215V, P108.223G, P111.24HD. PJ was supported by the Polish National Science Center through grant no. 2020/38/E/ST9/00395. This work is supported by the Belgo-Indian Network for Astronomy and astrophysics (BINA), approved by the International Division, Department of Science and Technology (DST, Govt. of India; DST/INT/BELG/P-09/2017) and the Belgian Federal Science Policy Office (BELSPO, Govt. of Belgium; BL/33/IN12).

Further Information

ORCID identifiers of the authors

0000-0002-0524-5328 (Priyanka JALAN)
0000-0001-5824-1040 (Vibhore NEGI)
0000-0002-7005-1976 (Jean SURDEJ)
0000-0002-5074-9998 (Céline BOEHM)
0000-0003-2559-408X (Ludovic DELCHAMBRE)
0000-0002-8760-6157 (Jakob Sebastian DEN BROK)
0000-0003-0699-7019 (Dougal DOBIE)
0000-0003-0228-6594 (Andrew DRAKE)
0000-0003-4843-8979 (Christine DUCOURANT)
0000-0002-0603-3087 (S. George DJORGOVSKI)
0000-0002-8541-0476 (Laurent GALLUCCIO)
0000-0002-3168-0139 (Matthew J. GRAHAM)
0000-0002-3469-5133 (Jonas KLÜTER)

0000-0002-2308-6623 (Alberto KRONE-MARTINS)
0000-0003-2242-0244 (Ashish A. MAHABAL)
0000-0002-2686-438X (Tara MURPHY)
0000-0001-6809-2536 (Anna NIERENBERG)
0000-0003-3739-4288 (Sergio SCARANO)
0000-0003-1407-6607 (Joseph SIMON)
0000-0003-4771-7263 (Eric SLEZAK)
0000-0001-6116-2095 (Dominique SLUSE)
0000-0002-8052-7763 (Carolina SPÍNDOLA-DUARTE)
0000-0003-2686-9241 (Daniel STERN)
0000-0002-6806-6626 (Ramachrisna TEIXERA)
0000-0002-8365-7619 (Joachim WAMBSGANSS)

Author contributions

This work results from a long-term collaboration (GAIA-GRAL) to which all authors have made significant contributions.

Conflicts of interest

The authors declare no conflict of interest.

References

- Agnello, A., Lin, H., Kuropatkin, E., N Schechter, P. L., Morishita, T., Motta, V., Rojas, K., Treu, T., Amara, A., Auger, M. W., Courbin, F., Fassnacht, C. D., Frieman, J., More, A., Marshall, P. J., McMahon, R. G., Meylan, G., Suyu, S. H., Glazebrook, K., Morgan, N., Nord, B., Abbott, T. M. C., Abdalla, F. B., Annis, J., Bechtol, K., Benoit-Lévy, A., Bertin, E., Bernstein, R. A., Brooks, D., Burke, D. L., Rosell, A. C., Carretero, J., Cunha, C. E., D’Andrea, C. B., da Costa, L. N., Desai, S., Drlica-Wagner, A., Eifler, T. F., Flaugher, B., García-Bellido, J., Gaztanaga, E., Gerdes, D. W., Gruen, D., Gruendl, R. A., Gschwend, J., Gutierrez, G., Honscheid, K., James, D. J., Kuehn, K., Lahav, O., Lima, M., Maia, M. A. G., March, M., Menanteau, F., Miquel, R., Ogando, R. L. C., Plazas, A. A., Sanchez, E., Scarpine, V., Schindler, R., Schubnell, M., Sevilla-Noarbe, I., Smith, M., Soares-Santos, M., Sobreira, F., Suchyta, E., Swanson, M. E. C., Tarle, G., Tucker, D. and Wechsler, R. (2018) DES meets Gaia: discovery of strongly lensed quasars from a multiplet search. *MNRAS*, 479(4), 4345–4354. <https://doi.org/10.1093/mnras/sty1419>.
- Bailer-Jones, C. A. L., Fouesneau, M. and Andrae, R. (2019) Quasar and galaxy classification in Gaia Data Release 2. *MNRAS*, 490(4), 5615–5633. <https://doi.org/10.1093/mnras/stz2947>.
- Bechtold, J. and Yee, H. K. C. (1995) High Spatial Resolution Spectroscopy of the Lyman-alpha Absorption Towards the Gravitational Lens System B1422+2309. *AJ*, 110, 1984. <https://doi.org/10.1086/117664>.

- Blandford, R. D. and Narayan, R. (1992) Cosmological applications of gravitational lensing. *ARA&A*, 30, 311–358. <https://doi.org/10.1146/annurev.astro.30.1.311>.
- Cao, S., Biesiada, M., Gavazzi, R., Piórkowska, A. and Zhu, Z.-H. (2015) Cosmology with Strong-lensing Systems. *ApJ*, 806(2), 185. <https://doi.org/10.1088/0004-637X/806/2/185>.
- Creevey, O. L., Sordo, R. and Pailler, F. (2023) Gaia Data Release 3. Astrophysical parameters inference system (Apsis). I. Methods and content overview. *A&A*, 674, A26. <https://doi.org/10.1051/0004-6361/202243688>.
- de Souza, R. E., Krone-Martins, A., dos Anjos, S., Ducourant, C. and Teixeira, R. (2014) Detection of galaxies with Gaia. *A&A*, 568, A124. <https://doi.org/10.1051/0004-6361/201423514>.
- Delchambre, L. (2018) Determination of astrophysical parameters of quasars within the Gaia mission. *MNRAS*, 473(2), 1785–1800. <https://doi.org/10.1093/mnras/stx2417>.
- Delchambre, L., Krone-Martins, A. and Wertz, O. (2019) Gaia GraL: Gaia DR2 Gravitational Lens Systems. III. A systematic blind search for new lensed systems. *A&A*, 622, A165. <https://doi.org/10.1051/0004-6361/201833802>.
- Dolan, J. F., Michalitsianos, A. G., Nguyen, Q. T. and Hill, R. J. (2000) Ultraviolet Spectral Variability and the Ly α Forest in the Lensed Quasar Q0957+561. *ApJ*, 539(1), 111–123. <https://doi.org/10.1086/309206>.
- Ducourant, C., Wertz, O. and Krone-Martins, A. (2018) Gaia GraL: Gaia DR2 gravitational lens systems. II. The known multiply imaged quasars. *A&A*, 618, A56. <https://doi.org/10.1051/0004-6361/201833480>.
- Efstathiou, G., Sutherland, W. J. and Maddox, S. J. (1990) The cosmological constant and cold dark matter. *Natur*, 348(6303), 705–707. <https://doi.org/10.1038/348705a0>.
- Finet, F. and Surdej, J. (2016) Multiply imaged quasi-stellar objects in the Gaia survey. *A&A*, 590, A42. <https://doi.org/10.1051/0004-6361/201425411>.
- Hubble, E. (1929) A Relation between Distance and Radial Velocity among Extra-Galactic Nebulae. *PNAS*, 15(3), 168–173. <https://doi.org/10.1073/pnas.15.3.168>.
- Jimenez, R., Verde, L., Treu, T. and Stern, D. (2003) Constraints on the Equation of State of Dark Energy and the Hubble Constant from Stellar Ages and the Cosmic Microwave Background. *ApJ*, 593(2), 622–629. <https://doi.org/10.1086/376595>.
- Kelly, P. L., Rodney, S., Treu, T., Oguri, M., Chen, W., Zitrin, A., Birrer, S., Bonvin, V., Dessart, L., Diego, J. M., Filippenko, A. V., Foley, R. J., Gilman, D., Hjorth, J., Jauzac, M., Mandel, K., Millon, M., Pierel, J., Sharon, K., Thorp, S., Williams, L., Broadhurst, T., Dressler, A., Graur, O., Jha, S., McCully, C., Postman, M., Schmidt, K. B., Tucker, B. E. and von der Linden, A. (2023) Constraints on the Hubble constant from supernova Refsdal’s reappearance. *Sci*, 380(6649), abh1322. <https://doi.org/10.1126/science.abh1322>.

- Krone-Martins, A., Delchambre, L. and Wertz, O. (2018) Gaia GraL: Gaia DR2 gravitational lens systems. I. New quadruply imaged quasar candidates around known quasars. *A&A*, 616, L11. <https://doi.org/10.1051/0004-6361/201833337>.
- Krone-Martins, A., Ducourant, C. and Teixeira, R. (2013) Pushing the limits of the Gaia space mission by analyzing galaxy morphology. *A&A*, 556, A102. <https://doi.org/10.1051/0004-6361/201219697>.
- Krone-Martins, A., Graham, M. J. and Stern, D. (2019) Gaia GraL: Gaia DR2 Gravitational Lens Systems. V. Doubly-imaged QSOs discovered from entropy and wavelets. arXiv e-prints, arXiv:1912.08977.
- Lemaître, G. (1927) Un Univers homogène de masse constante et de rayon croissant rendant compte de la vitesse radiale des nébuleuses extra-galactiques. *ASSB*, 47, 49–59.
- Lemon, C. A., Auger, M. W. and McMahon, R. G. (2019) Gravitationally lensed quasars in Gaia - III. 22 new lensed quasars from Gaia data release 2. *MNRAS*, 483(3), 4242–4258. <https://doi.org/10.1093/mnras/sty3366>.
- Lemon, C. A., Auger, M. W., McMahon, R. G. and Ostrovski, F. (2018) Gravitationally lensed quasars in Gaia - II. Discovery of 24 lensed quasars. *MNRAS*, 479(4), 5060–5074. <https://doi.org/10.1093/mnras/sty911>.
- Lotze, K.-H. and Simionato, S. (2022) Henry Cavendish on Gravitational Deflection of Light. *AnP*, 534(7), 2200102. <https://doi.org/10.1002/andp.202200102>.
- Perlmutter, S., Aldering, G., Goldhaber, G. a. and Project, T. S. C. (1999) Measurements of Ω and Λ from 42 High-Redshift Supernovae. *ApJ*, 517(2), 565–586. <https://doi.org/10.1086/307221>.
- Rauch, M., Sargent, W. L. W., Barlow, T. A. and Carswell, R. F. (2001) Small-Scale Structure at High Redshift. III. The Clumpiness of the Intergalactic Medium on Subkiloparsec Scales. *ApJ*, 562(1), 76–87. <https://doi.org/10.1086/323523>.
- Refsdal, S. (1964) On the possibility of determining Hubble’s parameter and the masses of galaxies from the gravitational lens effect. *MNRAS*, 128, 307. <https://doi.org/10.1093/mnras/128.4.307>.
- Riess, A. G., Filippenko, A. V. and Challis, P. (1998) Observational Evidence from Supernovae for an Accelerating Universe and a Cosmological Constant. *AJ*, 116(3), 1009–1038. <https://doi.org/10.1086/300499>.
- Stern, D., Djorgovski, S. G., Krone-Martins, A., Sluse, D., Delchambre, L., Ducourant, C., Teixeira, R., Surdej, J., Boehm, C., den Brok, J., Dobie, D., Drake, A., Galluccio, L., Graham, M. J., Jalan, P., Klüter, J., Le Campion, J. F., Mahabal, A., Mignard, F., Murphy, T., Nierenberg, A., Scarano, J., S., Simon, J., Slezak, E., Spindola-Duarte, C. and

- Wambsganss, J. (2021) Gaia GraL: Gaia DR2 Gravitational Lens Systems. VI. Spectroscopic Confirmation and Modeling of Quadruply Imaged Lensed Quasars. *ApJ*, 921(1), 42. <https://doi.org/10.3847/1538-4357/ac0f04>.
- Surdej, J. and Refsdal, S. (1994) Gravitational Lensing as a Tool: Future Observational Prospects, pp. 409–419. Springer Netherlands, Dordrecht. https://doi.org/10.1007/978-94-011-0794-5_40.
- Tsalmantza, P., Karamelas, A. and Kontizas, M. (2012) A semi-empirical library of galaxy spectra for Gaia classification based on SDSS data and PÉGASE models. *A&A*, 537, A42. <https://doi.org/10.1051/0004-6361/201117125>.
- Tzanavaris, P. and Carswell, R. F. (2003) Size estimates for intervening CIV absorbers from high-resolution spectroscopy of APM 0827+5255. *MNRAS*, 340(3), 937–948. <https://doi.org/10.1046/j.1365-8711.2003.06355.x>.
- Walsh, D., Carswell, R. F. and Weymann, R. J. (1979) 0957+561 A, B: twin quasistellar objects or gravitational lens? *Natur*, 279, 381–384. <https://doi.org/10.1038/279381a0>.
- Wertz, O., Stern, D. and Krone-Martins, A. (2019) Gaia GraL: Gaia DR2 gravitational lens systems. IV. Keck/LRIS spectroscopic confirmation of GRAL 113100-441959 and model prediction of time delays. *A&A*, 628, A17. <https://doi.org/10.1051/0004-6361/201834573>.
- Zwicky, F. (1937) Nebulae as Gravitational Lenses. *PhRv*, 51(4), 290–290. <https://doi.org/10.1103/PhysRev.51.290>.